

Zircaloy-4 ISCC

ISCC Properties of Zircaloy-4 Cladding

150

Zircaloy-4(Zry-4) 가	ISCC(iodine-induced stress corrosion cracking)
	Zry-4
ISCC	ISCC 623°K, iodine 10 ⁻³ g/cm ²
100	가 SEM
ISCC	K _I (stress intensity factor)
,	K _{I,ISCC} (threshold stress intensity factor)
.	

Abstract

An equipment of inducing an internal, longitudinal fatigue crack in a tube was designed and manufactured. Using this equipment, the Zircaloy-4 specimens, which had been fatigue-cracked at internal surface for evaluating their iodine-induced stress corrosion cracking (ISCC), were prepared. Tube pressurization tests were conducted at 623°K and the iodine concentration of 10⁻³ g/cm². The K_I (stress intensity factor) and crack propagation velocity were evaluated using the depth of ISCC crack measured by scanning electron microscope (SEM). From the relationship between the K_I and crack propagation velocity, K_{I,ISCC} (threshold stress intensity factor) of Zircaloy-4 cladding was estimated.

1.

1970
pellet cladding interaction)

/

(PCI :

(SCC : stress corrosion cracking)

SCC

ISCC (iodine-induced SCC)

가

가

가

ISCC

가

가

PCI

Zr-liner

PWR

BWR

가

ISCC

가

(stress intensity factor)

K_{ISCC}

DCB

ASTM

가

가

ISCC

가가

DB

K_{ISCC}

K_{ISCC}

ISCC

가

ISCC

PWR

Zircaloy-4

K

2.

2.1

Lemaignan[8]

가

Fig.1

Lemaignan

13 cm

Zircaloy-4

0.12 mm,

Instron 8516

sine wave

가

5Hz

5000 ~ 16000

가

ISCC

2.2 ISCC

Fig.2

ISCC

90Mpa

600

/

P&I

4

/

He 가 가 autoclave Ar
 가
 on-line PC Fig 3
 UM 330 9 , RS485 UT 320
 RS-converter, controller,
 PCMCIA Multi-port

2.3

8.36 mm, 0.57 mm Zircaloy-4 13 cm
 iodine ISCC Fig. 2
 Aldrich 350 가 iodine 가 , 10^{-3} g/cm²
 99.99% iodine ISCC 가
 100 가
 ISCC ISCC (SEM)

3.

3.1 pre-crack Fig.4

가 가
 가 가
 Fig.5 30 kg 0.12 mm 5Hz
 가 Fig 6 16,000 cycle 가
 350 2 가
 a/t K_I 가 Fig. 7
 (a/t)
 가

3.2 Stress Intensity Factor

ISCC 가 KISCC
 가 DCB ASTM 가
 가 가 Plane strain
 [9].

$$K_I \langle \sigma_y (3\pi t / 5) \rangle^{1/2}$$

σ_y , t, 570 μm , $\sigma_y =$
 220MPa $K_I < 7.2 \text{ MPa m}^{1/2}$ 가 Newman
 Fig. 4 가 가 P K_I
 [10]

$$K_I = \frac{pR}{t} \sqrt{\frac{\pi a}{Q}} F\left(\frac{a}{c}, \frac{a}{t}, \frac{t}{R}, \phi\right)$$

p = internal pressure on the tube
 R = inner radius of the tube
 t = tube wall thickness
 a = depth of surface crack
 Q = shape factor for an elliptical crack = $1 + 1.464(a/c)^{1.65}$
 c = half-length of surface crack
 ϕ = parametric angle of elliptical crack

Fig.8 $t/R = 0.13$, $\phi = \pi/2$ K_I
 a/t a/c f_c

3.3 K_{ISCC}

Fig.9 Fig.10 ISCC 2000 SEM 가
 ISCC 가 100 0.21 mm
 $5.8 \times 10^{-7} \text{ mm/sec}$ $a/c = 0.3$,
 $a/t = 0.5$ 14.7 MPa K_I 2.94
 Fig. 11 Zircaloy-4 K_{ISCC} 3.3 $\text{MPa m}^{1/2}$

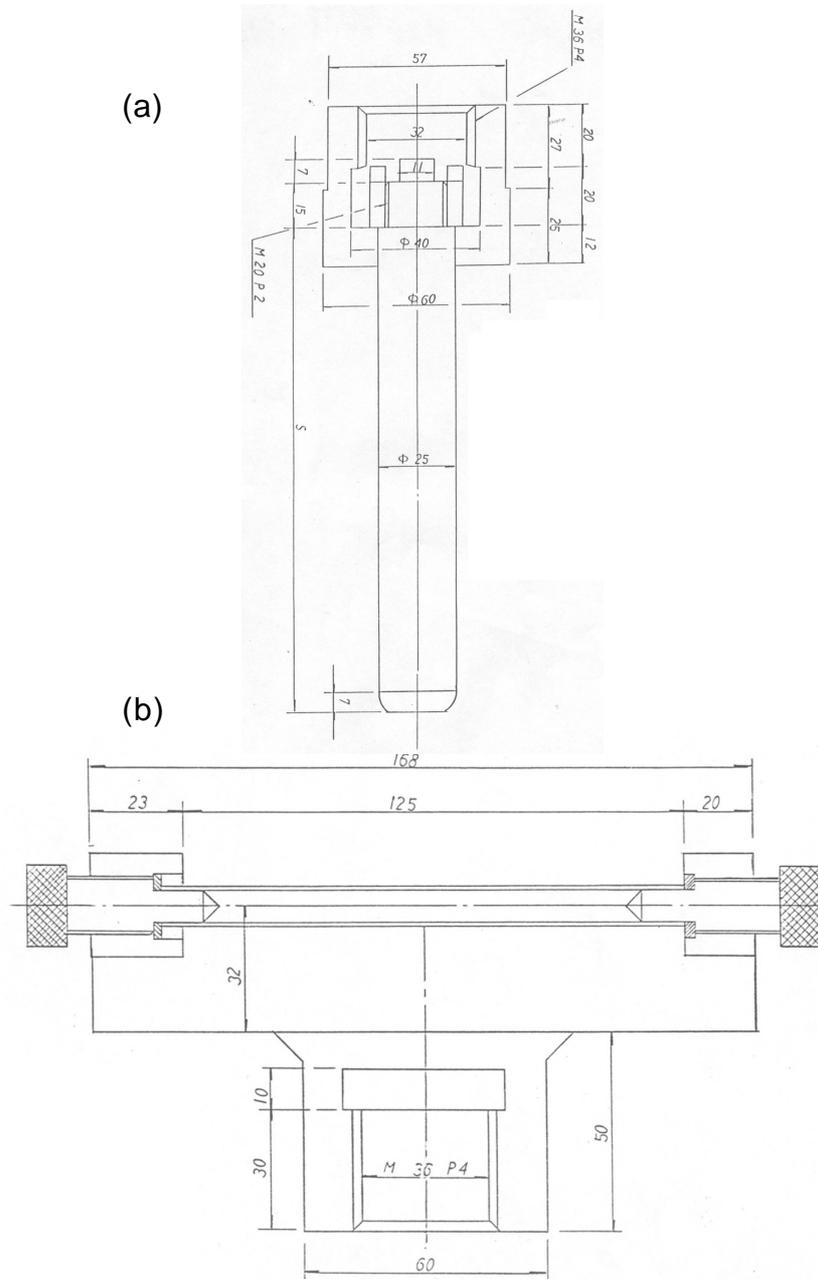


**Fig. 1 Loading cell for making the fatigue pre -crack;
 (a) upper part and (b) lower part**

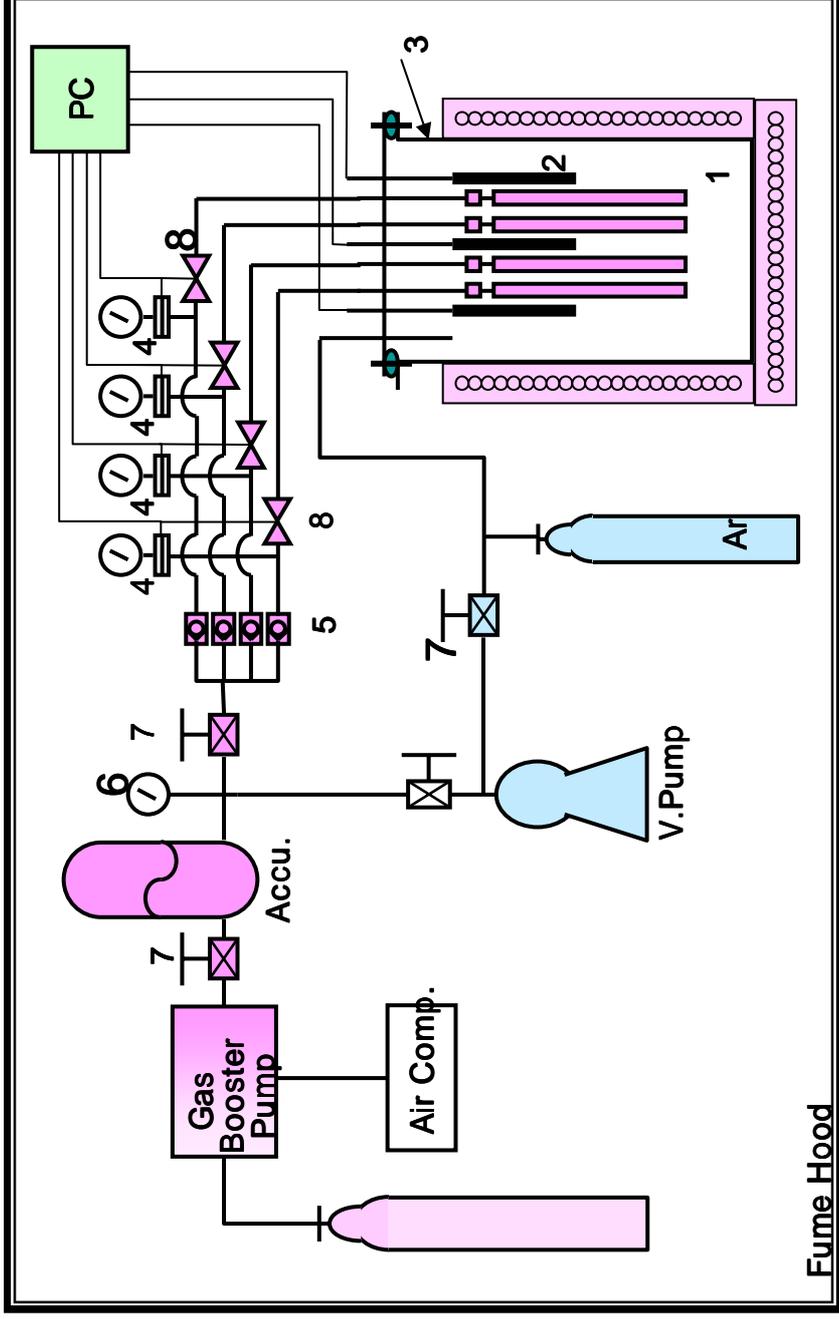


Fig. 2. Schematic drawing of the ISCC Testing Facility

- 1: Specimens, 2: Thermocouple, 3: SS Liner (100φ X 300L),
- 4: High Pressure Gauges & Transducers, 5: High Pressure Regulators,
- 6: High Pressure Gauge, 7: High Pressure Valves, 8: Automatic Valves

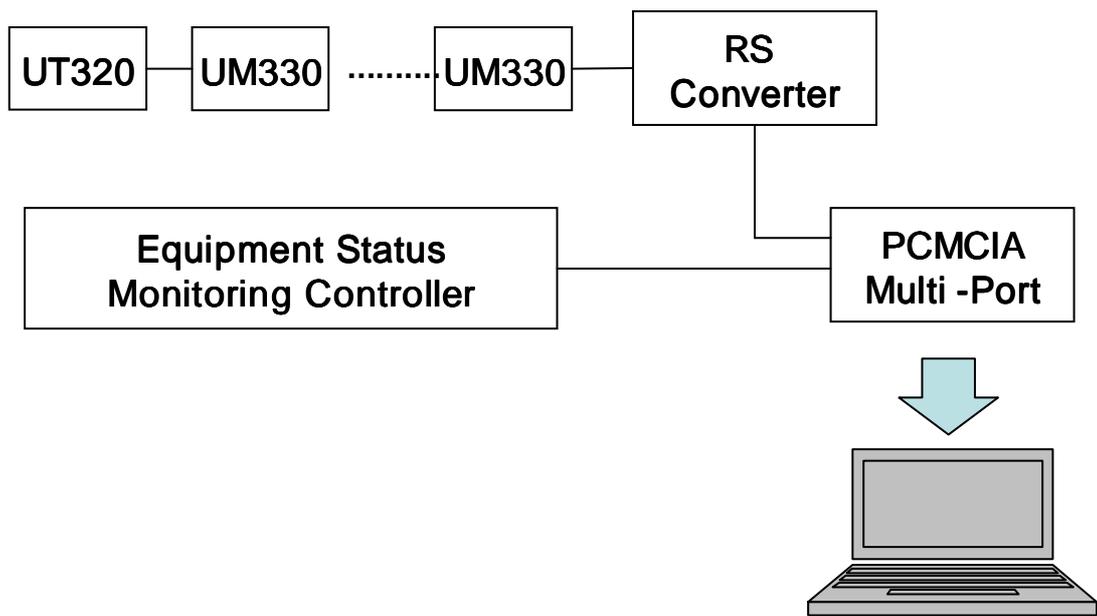


Fig. 3. Control and indication system

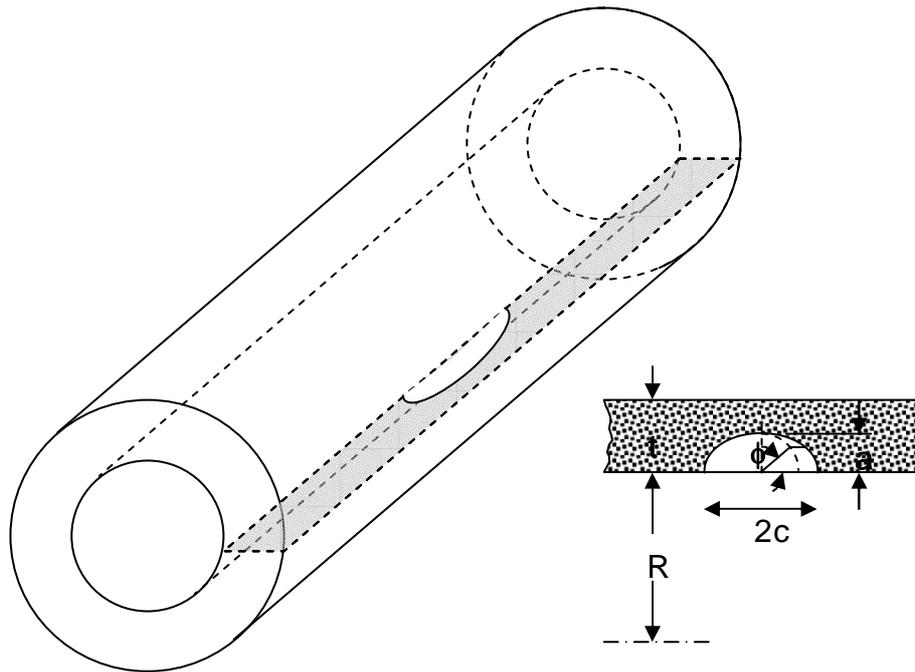


Fig. 4. Surface crack in an internally pressurized cylinder

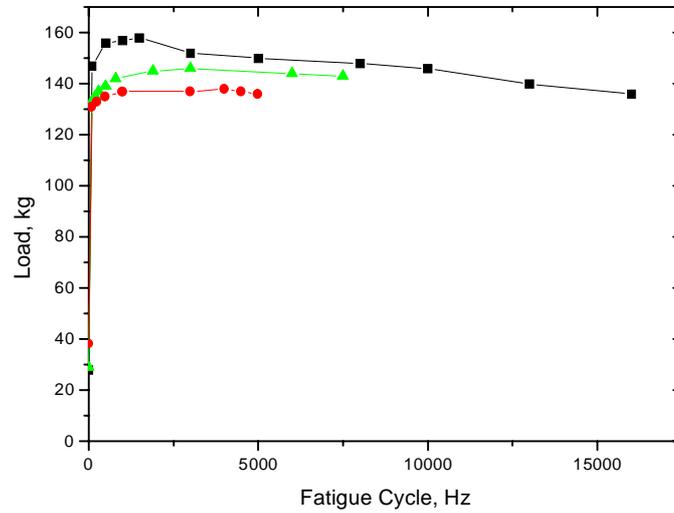


Fig. 5. Load vs. frequency plots

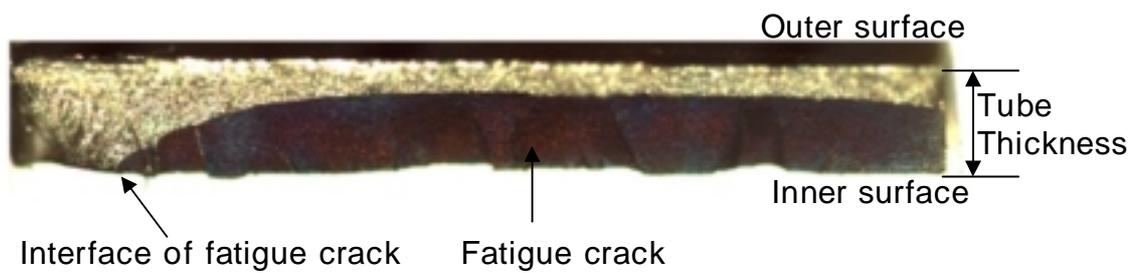


Fig. 6. Cross-section of pre-crack showing the depth of fatigue crack (70% of total tube thickness).

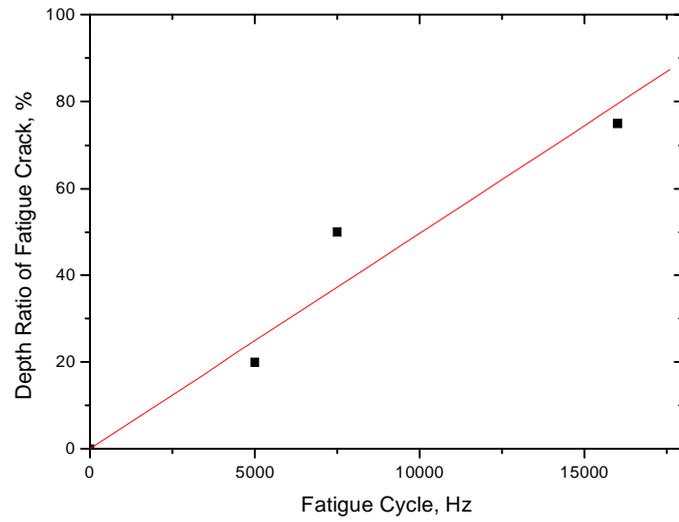


Fig. 7. Depth ratio of fatigue crack vs. fatigue cycle plots.

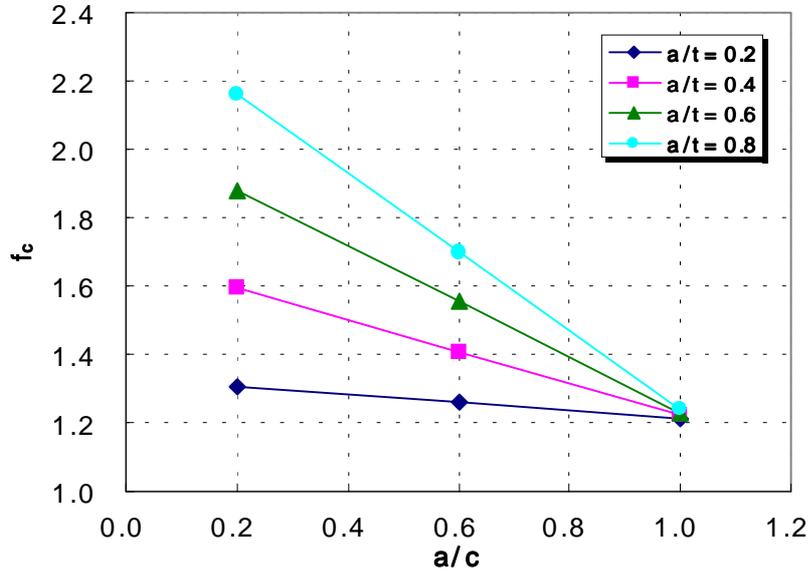


Fig. 8. Boundary -correction factor for a surface crack in a pressurized tube ($t/R=0.13$)

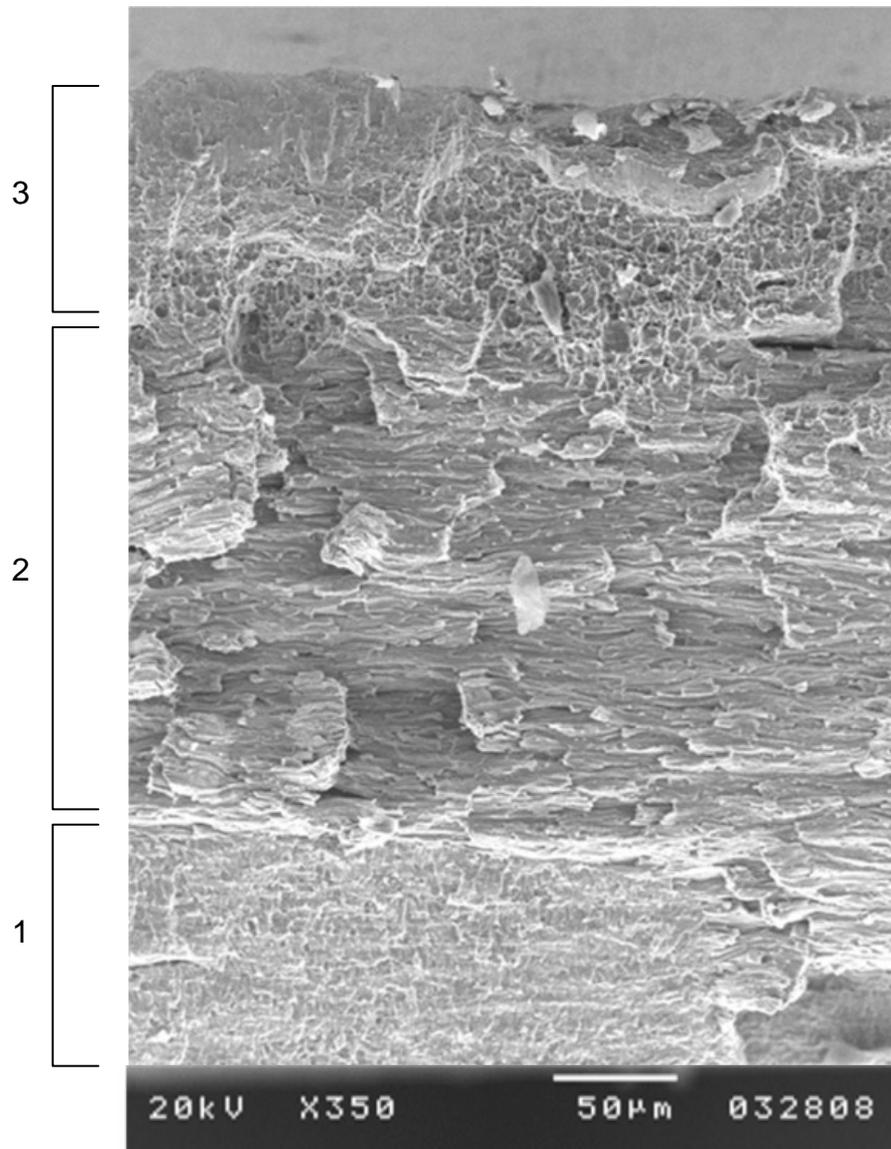


Fig. 9. Fracture surface in the defect area of a specimen tested for; 1 – fatigue crack; 2 – ISCC; 3 – ductile overload

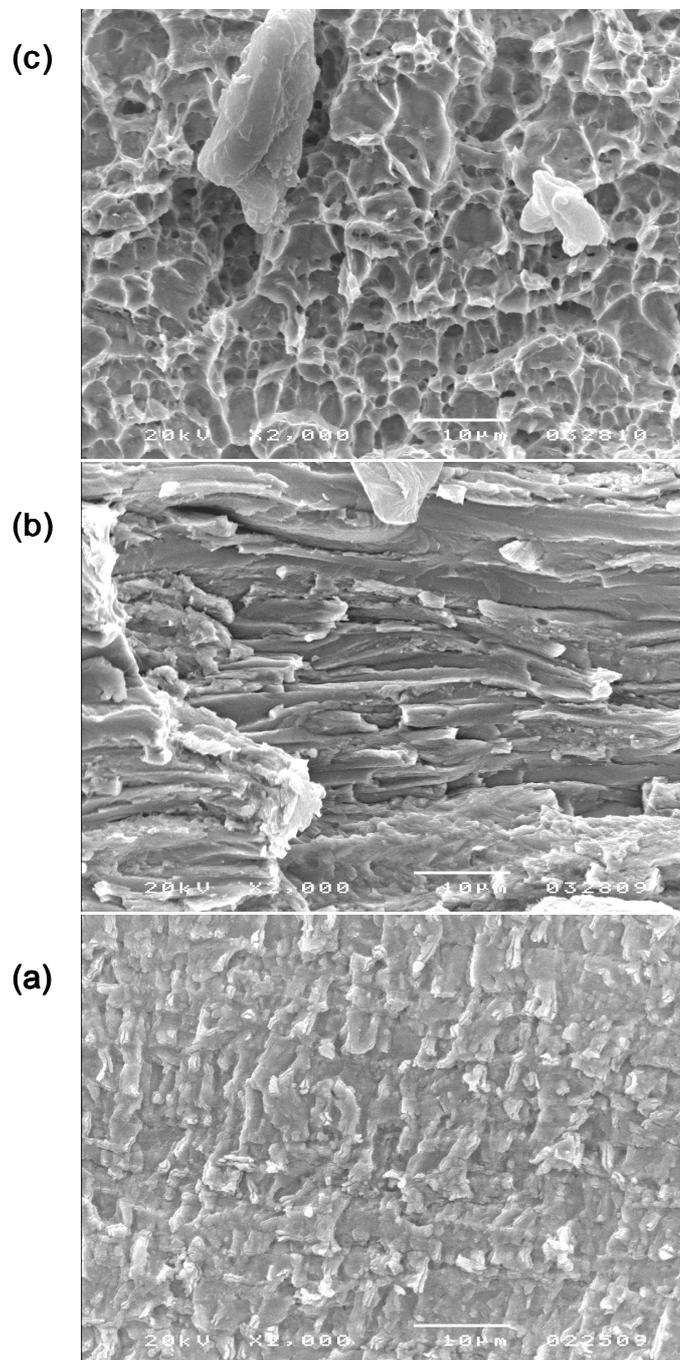


Fig. 10. Detailed fracture surface in the defect area of a specimen tested for (a) fatigue crack; (b) ISCC; (c) ductile overload

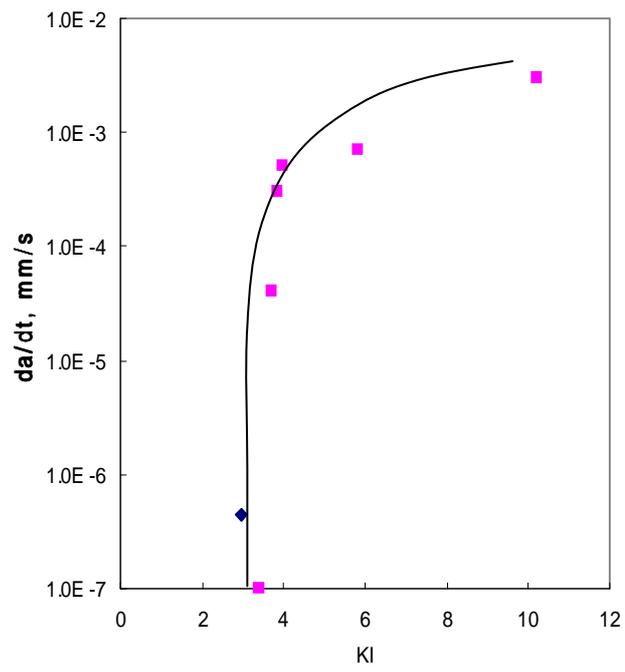


Fig. 11. Crack propagation rate versus stress intensity factor for Zircaloy -4 claddings